Research Article | Vol. 32, No. 6 / 11 Mar 2024 / Optics Express 10348
Optics EXPRESS

Chromatic changes in vision with diffractive ophthalmic optics

LAURA CLAVÉ,[1,2,*] MIGUEL FARIA-RIBEIRO,[3] AND MARIA S. MILLAN[1]

[1] *Departament d'Òptica i Optometria, Universitat Politècnica de Catalunya-BarcelonaTech, Violinista Vellsolà 37, 08222 Terrassa, Spain*
[2] *Consorci Sanitari del Maresme, Hospital de Mataró, Carretera de Cirera 230, 08304 Mataró, Spain*
[3] *Physics Center of Minho and Porto Universities, University of Minho, 4710-057 Braga, Portugal*
[*] *laura.clave@upc.edu*

Abstract: Diffractive optics is a valuable technique for designing presbyopia-correcting lenses, but its effectiveness is wavelength-dependent. This study investigates the spatio-chromatic alterations in visual resolution associated with diffractive multifocal lenses by using non-invasive, removable diffractive bifocal contact lenses. The study combines theoretical analysis, numerical simulation, and clinical intra-observer experiments to assess visual acuity under various lighting conditions. Results demonstrate the introduction of spatio-chromatic asymmetry and a change in visual acuity under red and blue lights, depending on the operating diffraction order employed in the lens design. The energy distribution of the diffractive contact lens studied favors resolution under red illumination at far distances and under blue illumination at near distances. These findings are consistent with computational simulations and provide insights into the visual changes induced by diffractive ophthalmic lenses.

1. Introduction

Diffractive profiles [1] have been successfully incorporated into ophthalmic optics to correct presbyopia by forming multiple coaxial images. Diffractive multifocal ophthalmic lenses aim to provide presbyopic patients with spectacle-independent clear vision at different distances. Straightforward applications can be found in intraocular lens (IOL) and contact lens (CL) designs [2–4], with varying levels of development and acceptance in modern clinical practice.

Hybrid refractive-diffractive multifocal lenses use two or more diffraction orders to focus light at different distances. In a basic bifocal design, the zeroth diffraction order, which does not modify the refractive power of the carrier lens, is used for far vision, and the first diffraction order, which adds the optical power required to see closer objects [2,5], is used for near vision. Other designs use different diffraction orders for different purposes [6,7].

Optical theory predicts that the power and energy efficiency of diffraction orders are both strongly wavelength-dependent, with the exception of the null power of the zero order, which exhibits no wavelength dependence. This is relevant in human vision, which typically operates under polychromatic illumination. As in refractive lenses, the power variation with wavelength gives rise to longitudinal chromatic aberration (LCA). However, for diffractive lenses operating with the first diffraction order and higher, LCA is the opposite sign of that of refractive lenses. Therefore, it can be used to compensate for the LCA of the eye [8]. This property has been used to design hybrid refractive-diffractive IOLs with improved performance [9,10].

Comprehensive research, including mathematical analysis, optical experimentation, and physiological studies, has evaluated the effects of diffractive patterns embedded in ophthalmic optics on the LCA of the eye (see, for instance, [8,11–13]). It is important to note that human vision is highly tolerant of LCA [14].

#512212 https://doi.org/10.1364/OE.512212
Journal © 2024 Received 16 Nov 2023; revised 26 Jan 2024; accepted 26 Jan 2024; published 7 Mar 2024

Optics EXPRESS

The wavelength dependence of the energy efficiency distribution among diffraction orders has received less attention. Although proven mathematically [1,11] and experimentally on optical-bench [6,12,15], its effects on vision are often masked or overlooked due to the difficulty of testing them without the influence of other factors. Moreover, the prevalence of red and longer wavelengths in the far focus of diffractive bifocals designed to have equal efficiency in both orders under a green reference (e.g., 550 nm) has become controversial in clinical instrumentation, prior to being detected in vision. Near-infrared-based sensors such as automated refractometers and double-pass aberrometers, which use wavelengths ranging from 780 to 850 nm, could potentially make inaccurate evaluations of subjects wearing diffractive aids [8,16,17]. This issue has been recently addressed for various diffractive multifocal designs [18,19].

In vision, Łabuz et al. [20] measured the effects of a 580 nm high-pass orange/red filter on the visual acuity (VA) and contrast sensitivity of patients implanted with a low-add extended-depth-of-focus diffractive IOL that operated with the first and second diffraction orders for distance and intermediate vision, respectively. Compared to white light viewing, the orange/red filter did not improve far vision but had an adverse effect at the near and intermediate distances. More recently, Millan et al. [21] conducted a series of optical and clinical experiments to study the spatio-chromatic changes in patients implanted with diffractive IOLs and provided a physical rationale based on the optical design of the lens. They found that the visual quality under red (R) and blue (B) lights is asymmetrical when changing from distance to near vision for this type of pseudophakic subject. Additionally, the visual quality under R and B lights differs from the visual quality under white (W) light, which is similar to that under narrowband green (G) light (close to the design wavelength). Due to the invasive nature of IOL implantation and the irreversible visual condition of pseudophakic subjects, the VA assessments reported in [21] could not be compared to the natural vision of the same subjects.

In this cross-sectional study, we propose to use a non-invasively diffractive optical system incorporated into the human presbyopic eye, namely a diffractive contact lens. This way, we will be able to compare, even for each subject, their own W, R, G, and B VA outcomes in far and near vision in two conditions: with and without the diffractive CL. The latter condition will involve the use of ophthalmic (refractive) spectacle lenses for presbyopia correction. Such a comparison aims to better reveal the changes in spatio-chromatic vision that affect individuals with diffractive multifocal lenses. The experiment conducted here with multifocal diffractive CLs can be replicated preoperatively to IOL implantation, using a clinical visual simulator [22] to further guide IOL selection.

2. Materials

2.1. Diffractive contact lenses

We used hybrid refractive-diffractive bifocal CLs in this study. These were Pilkington Diffrax CLs, which are made of RGP (rigid gas permeable) material. Diffrax lens design uses the principles of refraction and diffraction, with the diffractive surface engraved in the rear surface to generate the addition power [23]. The diffractive surface consists of a series of small diffractive steps of the same height that introduce a maximum optical path difference equal to half a wavelength retardation for the design wavelength, i.e., a π rad phase shift modulation. Its implementation for a Diffrax lens type, with a π-step size for the wavelength λ_0 = 550 nm [24], is physically equivalent to the diffractive bifocal lens described by Cohen [3]. The lens operates with the zeroth order for distance vision and the first order for near vision. The incident light splits symmetrically between these orders (around 41% each) for the design wavelength, with the rest of the energy being directed to higher diffractive orders with indirect implications for the vision function. The diffractive zone has the appearance of a number of concentric rings in the central region of the lens aperture (Fig. 1). The lenses used in this work have 11 rings covering approximately the 5 mm (4.91 mm) central area of the lens, which provide a specified add power of +2.00 diopters

Optics EXPRESS

(D) [25] at the design wavelength (550 nm). The set of Diffrax CLs consisted of nine positive (+3.25 D) and nine negative (-3.25 D) distance spherical power, with a back radius of curvature ranging from 7.3 to 8.1 mm, in steps of 0.1 mm.

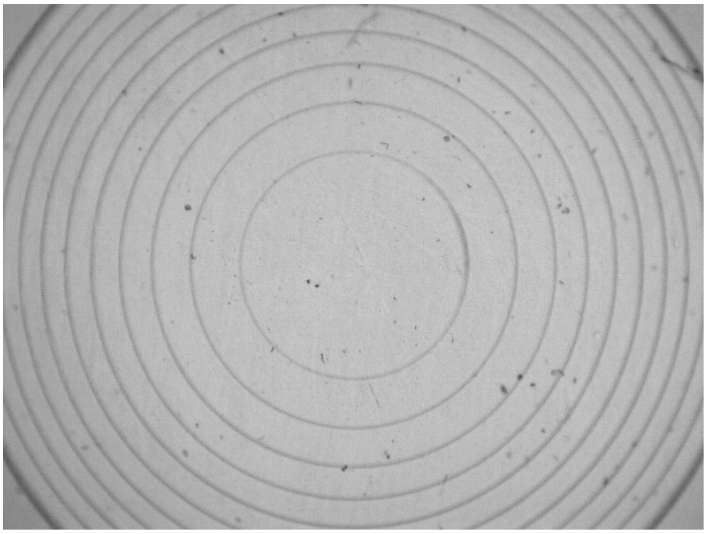

Fig. 1. Diffrax contact lens with 11 rings covering a 5 mm diameter central region.

2.2. Spectacle lenses

We used spectacle lenses (SL) from a trial set of common use in optometric examination (+/- 0.25 D steps).

3. Method

The method has two parts: an analytical description of the concept, including a numerical simulation, and a clinical experiment.

3.1. Concept

Let us consider the diffractive profile of a kinoform phase surface placed on the rear surface of a refractive (meniscus) CL. In paraxial approximation, the profile is parabolic [1]. The phase shift $\varphi(r)$ in radians induced at a point of radial coordinate r located in the m - zone (m=1, 2, 3. . .) is [3,26]

$$\varphi(r) = \frac{2\pi}{\lambda_0}(n_{CL} - n_T)h\left(m - \frac{r^2}{r_1^2}\right), \tag{1}$$

where λ_0 is the design wavelength in the free-space, n_{CL} and n_T the refractive indices of the contact lens material and the lacrimal fluid (tear), respectively, h is the maximum profile height ($h = \lambda_0/(n_{CL} - n_T)$ for a phase shift of 2π rad), and r_1 the radius of the first zone. The transmission function of the diffractive phase profile, $t(r) = \exp\{i\varphi(r)\}$, is periodic in r^2 with period r_1^2 (i.e., ${r_m}^2 = m{r_1}^2$), and can be expanded into a Fourier series. The Fourier coefficients C_j allow the calculation of the energy efficiency η_j of each diffraction order $j = 0, \pm1, \pm2, \ldots$ through the expression $\eta_j = C_j C_j^*$. In case of a step height that produces a maximum optical path difference

Optics EXPRESS

of $p\lambda_0$ (equivalent to a phase shift of $p2\pi$ rad), the energy efficiency for the j-diffraction order is

$$\eta_j(p) = \text{sinc}^2(\alpha p - j)\ , \tag{2}$$

where $\text{sinc}(x) = \sin(\pi x)/\pi x$. Parameter α of Eq. (2) is the fraction of 2π phase delay introduced for a wavelength λ other than the design wavelength λ_0, that is, $\alpha = (\lambda_0/\lambda) \times \{[n_{CL}(\lambda) - n_T(\lambda)]/[n_{CL}(\lambda_0) - n_T(\lambda_0)]\}$ [1]. In the context of materials with relative low dispersion, such as those of CL and tear, this parameter can be approximated by $\alpha = (\lambda_0/\lambda)$.

The optical power of the j-diffraction order is

$$P_{\text{add}}(\lambda,\ j) = \frac{j}{\alpha} P_{\text{add}}(\lambda_0,\ 1), \tag{3}$$

with $P_{\text{add}}(\lambda_0,\ 1) = 2\lambda_0/n_T r_1^2$. In the example of a bifocal diffractive profile [3], for the design wavelength λ_0 ($\alpha = 1$) and phase shift of π rad at the maximum step height ($p = 0.5$), Eq. (2) results in $\eta_0(0.5) = \eta_1(0.5) = 40.5\%$ for the zeroth and first orders. Interestingly, although the zeroth order does not contribute with any power no matter the wavelength (Eq. (3)), its energy efficiency does depend on the wavelength (Eq. (2)). For other diffraction orders, both the power and energy efficiency depend strongly on the wavelength (Eq. (2) and Eq. (3)).

The refractive power of the rear surface of the contact lens is $P_{\text{rear}} = (n_{CL} - n_T)/R$, where R is the back central optic radius of the base curve which is close to the apical radius of the anterior cornea surface. From Eq. (3), this power would keep unaffected by the zeroth diffraction order of the diffractive profile (far vision), whereas would be increased with the contribution of the first diffraction order up to $P_{\text{rear}} + P_{\text{add}}(\lambda,\ j)$ for near vision.

To further determine the optical performance of the diffractive component, we calculated the point spread function (PSF), more specifically, its peak irradiance variation along the optical axis. The 1D-complex amplitude function can be obtained from the light propagation in the far field approximation of scalar diffraction, described by Eq. (4) (except for global constants):

$$U(0,0,z) \propto \iint_{-\infty}^{+\infty} U_K(x,y,0)\exp\left\{i\frac{\pi(x^2+y^2)}{\lambda z}\right\}\text{d}x\text{d}y = \iint_A \exp\{i\varphi(r)\}\exp\left\{i\frac{\pi r^2}{\lambda z}\right\}\text{d}x\text{d}y, \tag{4}$$

where the field in the kinoform plane $U_K(x,y,0)$ equals the transmission function of the diffractive phase profile $t(r) = \exp\{i\varphi(r)\}$, the radius satisfies $r^2 = x^2 + y^2$, z is the propagation distance along the axis, and λ is the wavelength of the incident light. The integral of Eq. (4) is limited by the squared aperture A. It can be efficiently solved by means of Fourier transform. The normalized peak irradiance of the axial point of the PSF is given by

$$I(0,0,z) = \left(\frac{|U(0,\ 0,\ z)|}{A}\right)^2. \tag{5}$$

By varying λ, we evaluate the peak irradiance of the axial point of the PSF for different wavelengths, thereby studying the chromatic properties of the diffractive element in isolation.

For the numerical simulation, we wrapped a phase profile corresponding to a parabolic curve of +2.00 D for the design wavelength (550 nm) in 2π segments and halved it to obtain a diffractive phase profile with π-step size ($p = 0.5$) (Fig. 2). This profile splits light symmetrically into the zeroth and first diffraction orders, with approximately 40.5% of the incident energy each. We used MATLAB (The MathWorks, Inc., Natick, MA, USA) to evaluate the theoretical through-focus light distribution of the diffractive phase profile, simulated using the Diffrax CL design. The software uses Fourier optics principles to calculate the light distribution at different planes along its path after the light has been diffracted by the CL. The mathematical simulation is intended to illustrate the chromatic behavior of the diffractive CL and to facilitate a physical interpretation of the clinical results.

Optics EXPRESS

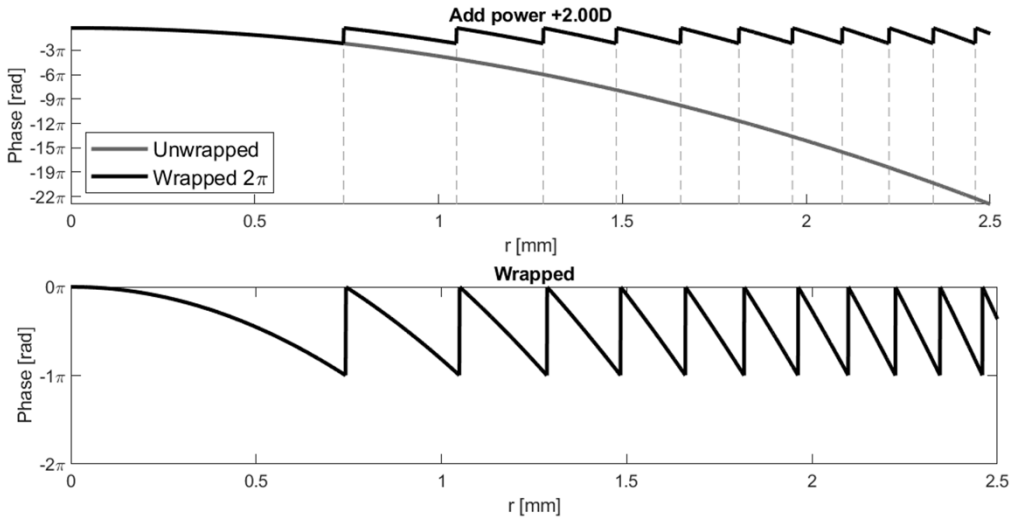

Fig. 2. Diffractive phase profile. Top: parabolic phase shift that induces +2.00 D addition power, both unwrapped and wrapped in 2π rad-steps. Bottom: 2π rad-wrapped profile halved, resulting in π-phase jumps.

3.2. Clinical experiment

We assessed VA in one eye of nine presbyopic phakic subjects aged 51-64 years (mean 56.5 years), following the tenets of the Declaration of Helsinki. Key inclusion criteria were refractive error (spherical equivalent) less than ±5.0 D, best distance-corrected VA better than 0.1 logMAR, and absence of ocular pathologies, prior refractive surgery, media opacities, and abnormal color vision.

Two high-contrast Landolt rings optotype charts were specifically designed to measure VA at far and near distances [27]. To avoid any learning effect during the assessment, three different versions of each chart were generated and randomly presented to the subjects. Since the optotype chart was positioned at 4.00 meters for distance vision, a + 0.25 D trial lens was incorporated into the manifest refraction. All subjects received SL compensation, if needed, to achieve optimal distance correction under white light. Near VA was tested by placing the corresponding charts approximately 45 to 50 cm from the subject.

To evaluate VA under lights of different spectral distributions, the chart was illuminated sequentially with white (W) light, and three narrowband color lights: green (G = 530 nm), red (R = 625 nm), and blue (B = 455 nm). Table 1 lists the specifications of the light-emitting diode (LED) sources.

Table 1. Light sources (Thorlabs, Inc., USA)[a]

Light	Manufacture model	λ (nm)	FWHM (nm)	CCT (K)
W	Thorlabs MCWHL5-LED	-	-	6500
G	Thorlabs M530L3-LED	530	33	-
R	Thorlabs M625L3-LED	625	18	-
B	Thorlabs M455L3-LED	455	18	-

[a]Peak wavelength λ (nm), full width at half maximum (FWHM), correlated colour temperature (CCT) (K).

Optics EXPRESS

The intensities of the LEDs were adjusted to ensure that the luminance reflected from the charts was constant for all three chromatic conditions during the assessment. The luminance was measured using a Mavolux 5032C photometer and set to 25.3 ± 0.1 cd/m^2. To minimize any potential confounding factors, the lighting conditions of the examination room were maintained at mesopic levels throughout the experiment. All examinations were conducted monocularly, assessing the same subject's eye under natural pupil conditions.

For each observer, the examination was performed in two stages:

Stage 1: VA assessment with spectacle lens

We evaluated far and near VA of each subject under successive W, R, G, and B illumination. The optical compensation to achieve the best corrected VA at far under W light was maintained to assess the far VA under the remaining R, G, and B illuminations. Spectacle addition was used to test near VA under W light and kept unchanged under the successive R, G, and B lights (Fig. 3(a)).

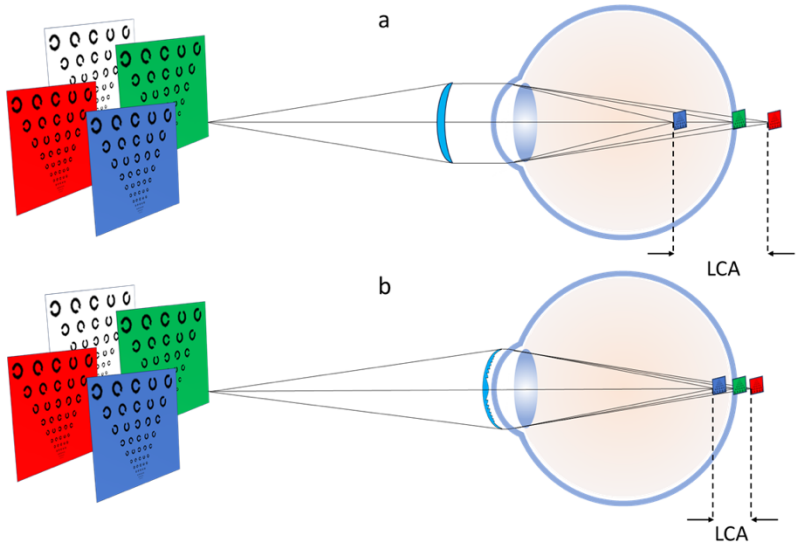

Fig. 3. Sketch of the near visual acuity assessment of a presbyopic eye under white, red, green, and blue illumination: (a) with the add power provided by a spectacle lens, (b) with the add power provided by the first diffraction order of a Diffrax contact lens. Longitudinal chromatic aberration (LCA) is approximately represented in both cases.

Stage 2: VA assessment with diffractive contact lens

An RGP Pilkington Diffrax diffractive CL was fitted following the manufacturer's instructions, which recommend selecting a lens with a back central optic radius 0.1 mm steeper than the flattest corneal radius of curvature [24]. The VA was examined in the same eye as the previous examination. After the stabilization of the CL in the observer's eye, a new refraction was performed to obtain the best corrected distance VA at 4.00 m with W light (again, a + 0.25 D trial lens was included in the manifest refraction). This refraction correction was maintained to assess the far VA under R, G, and B successive illumination. Next, we tested near VA under W, R, G, and B lights (Fig. 3(b)) without any further addition with SL and relied solely on the add power provided by the first diffraction order of the diffractive profile of the Diffrax CL.

Optics EXPRESS

4. Results

4.1. Numerical simulation

Figure 4 shows the computational simulation of the normalized irradiance distribution of the axial point of the PSF produced by the diffractive CL, with effective circular pupil of 5.0 mm, along the optical axis (also called through-focus). In this simulation, we iteratively varied the propagation distance (z) in Eqs. (4) and (5) and calculated the normalized irradiance at each step. We converted the propagation distance into object vergence, expressed in diopters, and presented it on the abscissa axis (defocus) of Fig. 4. Therefore, the origin of defocus (0.0 D) represents an object positioned at infinity. We have considered the three peak wavelengths – R (625 nm), G (530 nm), and B (455 nm) – of the color LED sources (Table 1) used in the clinical experiment.

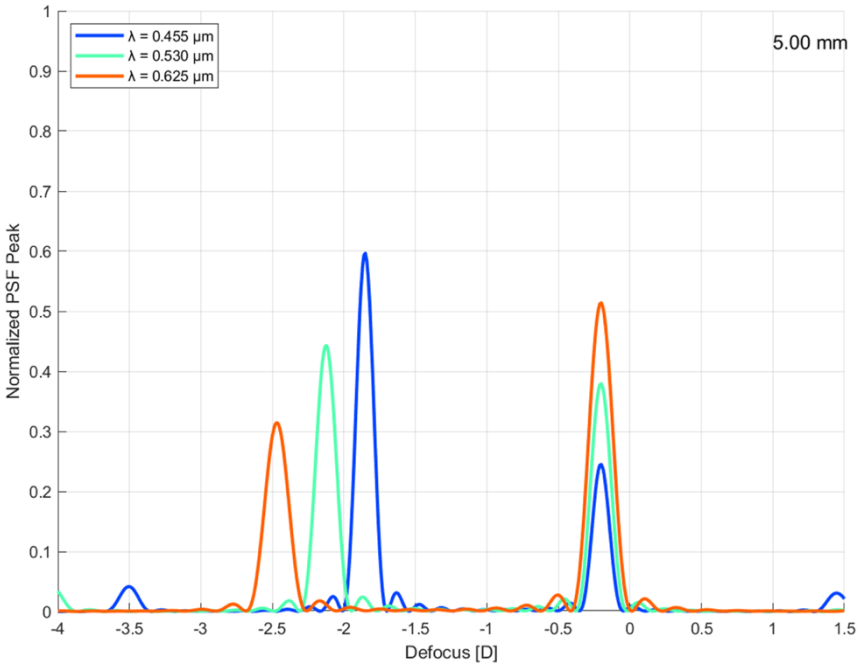

Fig. 4. Numerical simulation for a diffractive contact lens (Diffrax). R (625 nm), G (530 nm), and B (455 nm) normalized intensities of the axial point of the point spread function (PSF) versus defocus (D), with 0.0 D adjusted to the far focus for the design wavelength (550 nm). Pupil 5.0 mm.

Two intensity peaks for far and near vision, corresponding to the zeroth and first diffraction orders, respectively, are obtained with each wavelength (Fig. 4). In the zeroth order, the addition power is null for all wavelengths (Eq. (3)) and, hence, the diffractive phase profile does not contribute to LCA in this order. In the first order, however, LCA is produced by a chromatic difference of power (CDP) that can be calculated from Eq. (3),

$$CDP\ (\lambda_B, \lambda_R, j = 1) = P_{\text{add}}(\lambda_B,\ 1) - P_{\text{add}}(\lambda_R,\ 1)\ = -\frac{\lambda_R - \lambda_B}{\lambda_0} P_{\text{add}}(\lambda_0,\ 1) \tag{6}$$

which, with $P_{\text{add}}(\lambda_0,\ 1)$ = +2.00 D and the peak wavelength values for R and B lights (Table 1), turns out to be -0.62 D (i.e., higher optical power for R light than B). This CDP is opposite in sign to that of the human eye. The energy efficiency shows asymmetric differences between the zeroth and the first order for all three wavelengths ($\lambda_R, \lambda_G, \lambda_B$), as calculated from Eq. (2)

Optics EXPRESS

(Table 2). In the far focus, the R peak reaches the highest intensity and the B peak the lowest. The opposite happens in the near focus, where the most energetic peak is B and the lowest is R. The smallest asymmetry is observed for λ_G because it is closest to the design wavelength λ_0 = 550 nm. The peak values of the R, G, and B PSFs plotted in Fig. 4 agree well with the energy efficiency values of Table 2.

Table 2. Energy efficiency of the zeroth and first diffraction orders of the bifocal diffractive contact lens for the $(\lambda_0, \lambda_R, \lambda_G, \lambda_B)$ wavelengths. λ_0 is the design wavelength. Values calculated from Eq. (2) with p = 0.5.

	λ_0(550 nm)	λ_R(625 nm)	λ_G(530 nm)	λ_B(455 nm)
α [a]	1.00	0.880	1.038	1.209
		Energy efficiency (%)		
Zeroth order (j = 0)	40.5	50.5	37.5	24.9
First order (j = 1)	40.5	31.2	43.6	58.0

[a]Parameter $\alpha = (\lambda_0/\lambda)$ (see text).

Figure 5 illustrates the combined effect of the diffractive CL when paired with an eye. Dispersion was modeled using Cornu's hyperbolic formula for the refractive index of water as suggested by Le Grand in [28]. This approach yields a hyperbolic function describing the variation of absolute refractive error with wavelength, incorporating the coefficients reported by Thibos et al. (i.e., the refractive error in diopters can be modeled by the function $1.68524 - 0.63346/(\lambda - 0.21410)$, where wavelength λ is in microns) [29]. The positive LCA induced by the ocular media remains unaffected in the far focus (zeroth diffraction order), with $CPD(\lambda_B, \lambda_R)$ of approximately +1.08 D. In contrast, the LCA is effectively compensated and $CPD(\lambda_B, \lambda_R)$ reduced to less than a half (+0.47 D) in the near focus (first diffraction order). Figure 3 illustrates the LCA produced in near vision with spectacle correction (top) and with a diffractive CL operating with the first diffraction order (bottom). Comparing Figs. 4 and 5 reveals a shift in the positions of the R, G, and B peaks, while the relative energy efficiency distribution between far and near focus remains unchanged across all three wavelengths.

4.2. Clinical results

Table 3 shows the average far and near VA outcomes (mean ± standard deviation (SD)) obtained for the nine presbyopic eyes, under W, R, G, and B illuminations, in two observation conditions: with and without the diffractive lens. The latter condition represented SL correction alone, specifically incorporating the necessary addition for near vision. With one exception (near vision under B lighting, to be discussed later), the VA outcomes with the diffractive CL were generally worse than those obtained with SL correction under similar lighting conditions and vision distances.

Apart from Subject #5, all participants exhibited equal or better VA outcomes under W light compared to any of the narrowband R, G, or B illuminations, despite the influence of LCA (Table 3). This finding aligns with previously reported observations [21]. For comparative purposes, Fig. 6 presents the average VA differences obtained under R, G, and B lights relative to W light (labeled as R-W, G-W, and B-W) in both experimental observation conditions: with diffractive contact lens (CL) and with spectacle lens (SL) correction. Positive VA differences in logMAR units indicate worse VA under R, G, or B illumination compared to W light. Figure 7 displays the same information as Fig. 6 but for each individual subject's eye (#1, . . . #9).

In far vision (Fig. 6), the relative R-W, G-W, and B-W differences of VA exhibit consistent trends across the two experimental observation conditions: VA under B light is significantly worse than under R and G lights. However, in near vision, the observation condition plays a noteworthy role in influencing VA outcomes under the various R, G, and B illuminations. When

Optics EXPRESS

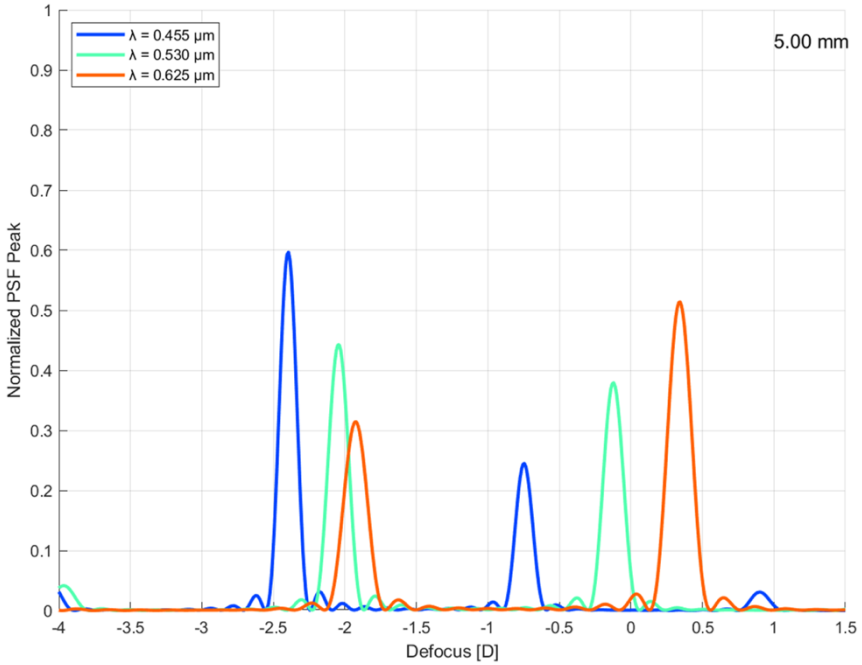

Fig. 5. Numerical simulation for a diffractive contact lens (Diffrax) combined with an eye. R (625 nm), G (530 nm), and B (455 nm) normalized intensities of the axial point of the point spread function (PSF) versus defocus (D), with 0.0 D adjusted to the far focus for the design wavelength (550 nm). Pupil 5.0 mm.

Table 3. Near and far VA (logMAR) for white (W), red (R), green (G) and blue (B) illuminations (mean ± SD).

		VA (logMAR)	
	Illumination	Spectacle lens	Contact lens
Near Vision	**W**	-0,09 ± 0,06	0,11 ± 0,10
	R	−0,08 ± 0,07	0,25 ± 0,18
	G	−0,04 ± 0,08	0,16 ± 0,12
	B	0,38 ± 0,12	0,17 ± 0,13
Far Vision	**W**	−0,07 ± 0,04	0,10 ± 0,11
	R	−0,02 ± 0,06	0,15 ± 0,09
	G	−0,02 ± 0,05	0,16 ± 0,08
	B	0,33 ± 0,05	0,46 ± 0,15

SL correction is employed, the VA results maintain a common trend with those observed in far vision, with significantly worse VA under B light compared to R and G lights. Notably, the introduction of the first diffraction order of the diffractive CL reverses this trend. VA under B light improves considerably (exhibiting a low relative difference compared to W light) and approaches the VA under G light. Conversely, VA under R light worsens markedly.

Optics EXPRESS

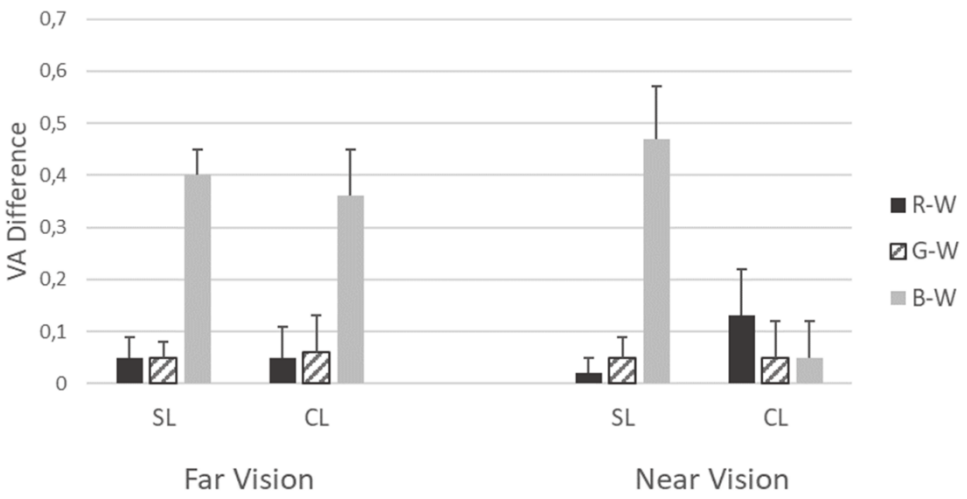

Fig. 6. Far and near VA differences (logMAR) obtained under R, G, B lights compared to W light in two observation conditions: with diffractive contact lens (CL) and with spectacle lens correction alone (SL). Bars represent mean + SD values.

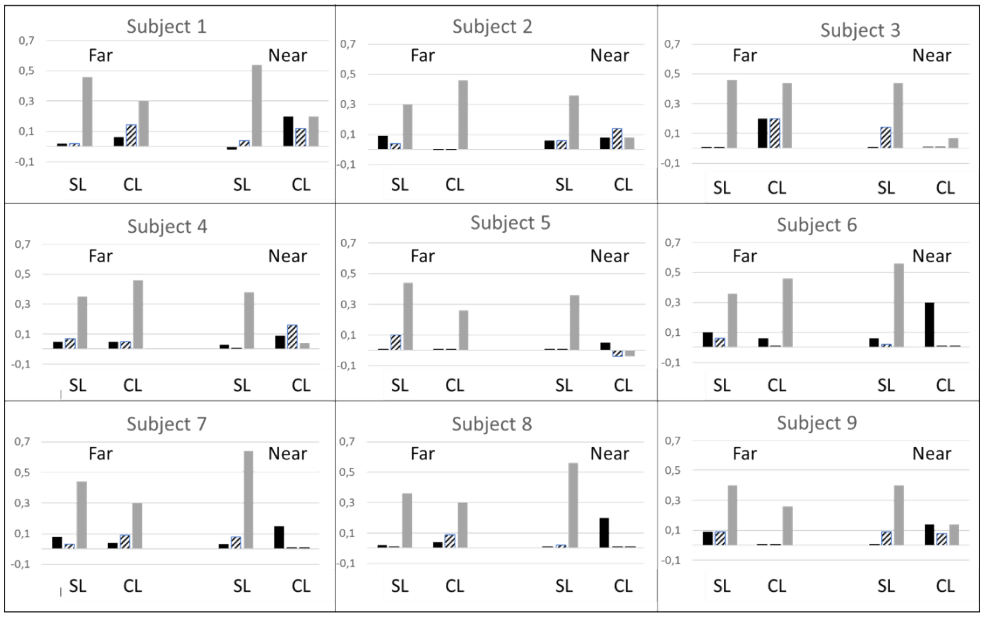

Fig. 7. Far and near VA differences (logMAR) for the nine individual subject's eyes (#1,. . . #9) obtained under R, G, B lights compared to W light in two observation conditions: with diffractive contact lens (CL) and with spectacle lens correction alone (SL). Colors and patterns have the same meaning as in Fig. 6 (Black: R-W; Striped: G-W; Grey: B-W).

Optics EXPRESS

5. Discussion

The chromatic changes in vision induced by diffractive ophthalmic optics (IOL and CL) used for presbyopia correction have primarily been studied in relation to LCA, despite the high tolerance of normal human vision to this aberration. The strong dependence of both the optical power and the energy efficiency of diffractive optical elements on wavelength prompted two of us to investigate their separate influences on vision following cataract surgery with implantation of a diffractive multifocal IOL [21]. An asymmetry in the visual spatial resolution assessed at far and near object distances was observed when the test was illuminated with either R or B lights. The physical explanation for this asymmetry lies in the wavelength dependence of the IOL's diffractive design, more specifically, its operative diffraction orders. In a previous study, Łabuz et al. [20] had already detected an adverse effect of an orange/red filter on visual acuity and contrast sensitivity at intermediate and near distances. These effects could not be solely attributed to LCA but were also influenced by the red predominance (higher energy efficiency) at far distance at the expense of near vision. In this work, we employed a reversible method by adapting a non-invasive lens, in the form of a diffractive CL, to further confirm and optically explain the asymmetry previously detected with diffractive IOLs. This approach allowed us to isolate the chromatic effects of the diffractive optics from other factors associated with cataract surgery and IOL implantation.

The diffractive bifocal design of the CL (design wavelength 550 nm) employed in this study utilizes the zeroth and first diffraction orders to achieve far and near vision, respectively. Consistent with the optical concept, our theoretical analysis predicts no contribution to ocular LCA under far vision conditions and partial compensation for ocular LCA under near vision conditions (Figs. 4 and 5). In terms of energy distribution, a clear predominance of R light is observed at far distances, while B light is dominant at near distances. As the lens bifocality produces coaxial images, contrast is invariably affected, with a more pronounced impact when a low-energy in-focus image is superimposed by an out-of-focus high-energy image. This phenomenon is evident when wearing the diffractive CL and observing the test either with B illumination at far distances or R illumination at near distances.

The impact of LCA is noticed in the final VA outcomes. The low energy efficiency of the CL in far focus under B light, coupled with the uncompensated ocular LCA, collectively contributes to the poor visual resolution for far vision under B illumination (Fig. 6). Conversely, near vision under B light benefits from both higher energy efficiency and partial compensation for ocular LCA by the CL's first diffraction order. This result significantly surpasses that obtained with refractive SL correction for near vision under B light.

The higher energy efficiency of the diffractive CL's zeroth order with R light does not provide a clear advantage in far vision under this illumination (Fig. 6). The VA outcomes in R light condition do not outperform, on average, those achieved with refractive SL. However, there is a clear detrimental effect of the CL's low energy efficiency at near under R light. In this situation, the VA outcomes are the worst compared to those obtained under G and B lights. Moreover, this result contrasts sharply with the excellent VA outcomes obtained under R light at near when using the addition provided by SL.

The inadequate performance of the diffractive CL at near distances under R light can solely be attributed to the unfavorable energy efficiency of the first diffraction order for this wavelength and cannot be ascribed to LCA effects. It is crucial to recall that LCA is partially compensated in the near focus. Furthermore, the effects of uncompensated ocular LCA, as experienced when using spectacle addition, appear to have minimal or no impact on the excellent VA achieved in near vision under R light.

Employing a removable optical device such as a CL provides the distinct advantage of facilitating intra-observer comparisons (the same subject's eye, with and without diffractive compensation).

Optics EXPRESS

These comparisons typically exhibit greater reliability than inter-observer comparisons (e.g., eyes from different subjects implanted with either a diffractive or non-diffractive IOL).

The intra-observer comparisons reported by our results further corroborate the alterations in spatio-chromatic vision experienced by individuals with diffractive multifocal lenses. The clinical findings obtained with presbyopic subjects align with the optical concept and the numerical simulation results concerning the chromatic performance of the CL. The experiment conducted here with multifocal diffractive CLs can be replicated preoperatively using a clinical visual simulator [22] to provide additional guidance in IOL selection.

This study is not without limitations. Except for near vision under B light, the VA outcomes with the CL were generally worse in both foci compared to those obtained with SL correction. The movement of the CL in the eye due to blinking or other design features might have influenced the results. We attempted to mitigate these circumstances by considering the relative VA differences with respect to W light in the two observation conditions. Subject's pupil size was not monitored during the experiment. However, since the diffractive design of the CL is not pupil-dependent within the central 5.0 mm region, the effect of pupil dynamics is expected to be minimal.

6. Conclusions

Diffractive optics is a highly effective method for generating multiple coaxial foci, making it valuable for designing presbyopia-correcting lenses (CLs and IOLs). One observed effect is the introduction of spatio-chromatic asymmetry in visual distance and a change in VA under R and B lights, depending on the operative diffraction orders of the lens design. In the case of the bifocal Diffrax CL studied in this work, which operates in the zeroth order for far vision and the first order for near vision, an energy predominance is observed for R illumination at far distances and for B illumination at near distances. This effect is consistent with previous results obtained with eyes implanted with multifocal diffractive IOLs and reported elsewhere. The spatio-chromatic visual changes produced by a removable diffractive CL in presbyopics have been compared with the natural vision corrected with SL and the results are consistent with the computational simulation.

Taking advantage of their non-invasive and removable nature, diffractive CLs serve as valuable tools for investigating intra-observer variations in color perception induced by diffractive patterns employed in ophthalmic lens designs.

Abbreviations

B Blue

CDP Chromatic difference of power

CL Contact lens

D Diopter

G Green

IOL Intraocular lens

LCA Longitudinal chromatic aberration

LED Light-emitting diode

PSF Point spread function

R Red

RGP Rigid gas permeable

Optics EXPRESS

SD Standard deviation

SL Spectacle lens

VA Visual acuity

W White

Funding. Agencia Estatal de Investigación (PID2020-114582RB-I00/AEI/10.13039/501100011033).

Acknowledgement. The authors acknowledge Prof. Norberto López Gil (Universidad de Murcia, Spain) for providing us with the set of Diffrax lenses.

Disclosures. The authors declare no conflicts of interest.

Data availability. Data underlying the results presented in this paper are not publicly available at this time but may be obtained from the authors upon reasonable request.

References

1. D. A. Buralli, G. M. Morris, and J. R. Rogers, "Optical performance of holographic kinoforms," Appl. Opt. **28**(5), 976–983 (1989).
2. A. L. Cohen, "Practical design of a bifocal hologram contact lens or intraocular lens," Appl. Opt. **31**(19), 3750–3754 (1992).
3. A. L. Cohen, "Diffractive bifocal lens designs," Opt. Vis. Sci. **70**(6), 461–468 (1993).
4. Ch.-Sh. Lee and M. J. Simpson, "Diffractive multifocal ophthalmic lens," U.S. Patent US5699142A, (16 December 1997).
5. M. J. Simpson, "Diffractive multifocal intraocular lens image quality," Appl. Opt. **31**(19), 3621–3626 (1992).
6. M. S. Millán and F. Vega, "Extended depth of focus intraocular lens: chromatic performance," Biomed. Opt. Express **8**(9), 4294–4309 (2017).
7. F. Vega, M. Valentino, F. Rigato, *et al.*, "Optical design and performance of a trifocal sinusoidal diffractive intraocular lens," Biomed. Opt. Express **12**(6), 3338–3351 (2021).
8. D. A. Atchison, M. Ye, A. Bradley, *et al.*, "Chromatic aberration and optical power of a diffractive bifocal contact lens," Optom. Vis. Sci. **69**(10), 797–804 (1992).
9. N. López-Gil and R. Montés-Micó, "New intraocular lens for achromatizing the human eye," J. Cataract Refract. Surg. **33**(7), 1296–1302 (2007).
10. H. A. Weeber and P. A. Piers, "Theoretical performance of intraocular lenses correcting both spherical and chromatic aberration," J. Refract. Surg. **28**(1), 48–52 (2012).
11. S. Ravikumar, A. Bradley, and L. N. Thibos, "Chromatic aberration and polychromatic image quality with diffractive multifocal intraocular lenses," J. Cataract Refract. Surg. **40**(7), 1192–1204 (2014).
12. M. S. Millán, F. Vega, and I. Ríos-López, "Polychromatic image performance of diffractive bifocal intraocular lenses: longitudinal chromatic aberration and energy efficiency," Invest. Ophthalmol. Visual Sci. **57**(4), 2021–2028 (2016).
13. M. Vinas, A. González-Ramos, C. Dorronsoro, *et al.*, "In vivo measurement of longitudinal chromatic aberration in patients implanted with trifocal diffractive intraocular lenses," J. Refract. Surg. **33**(11), 736–742 (2017).
14. N. Suchkov, E. J. Fernández, and P. Artal, "Impact of longitudinal chromatic aberration on through-focus visual acuity," Opt. Express **27**(24), 35935–35947 (2019).
15. M. S. Millán and F. Vega, "Through-focus energy efficiency and longitudinal chromatic aberration of three presbyopia-correcting intraocular lenses," Trans. Vis. Sci. Tech. **9**(12), 13 (2020).
16. F. Vega, M. S. Millán, N. Vila-Terricabras, *et al.*, "Visible versus near-infrared optical performance of diffractive multifocal intraocular lenses," Invest. Ophthalmol. Visual Sci. **56**(12), 7345–7351 (2015).
17. M. Faria-Ribeiro, "Letter to the Editor," Eye Vis. **8**(1), 47 (2021).
18. F. Vega, M. Faria-Ribeiro, J. Armengol, *et al.*, "Pitfalls of using NIR-based clinical instruments to test eyes implanted with diffractive intraocular lenses," Diagnostics **13**(7), 1259 (2023).
19. M. Faria-Ribeiro, J. M. González-Méijome, M. I. Pinho Ferreira, *et al.*, "Analysis of wavefront data obtained with a pyramidal sensor in pseudophakic eyes implanted with diffractive intraocular lenses," J. Refract. Surg. **39**(7), 438–444 (2023).
20. G. Łabuz, G. U. Auffarth, A. Özen, *et al.*, "The effect of a spectral filter on visual quality in patients with an extended-depth-of-focus intraocular lens," Am. J. Ophthal. **208**, 56–63 (2019).
21. M. S. Millán, L. Clavé, A. Torrents, *et al.*, "Spatio-chromatic vision with multifocal diffractive intraocular lens," Eye Vis. **10**(1), 32 (2023).
22. S. Marcos, E. Martinez-Enriquez, M. Vinas, *et al.*, "Simulating outcomes of cataract surgery: important advances in ophthalmology," Ann. Rev. Biomed. Eng. **23**(1), 277–306 (2021).
23. M. H. Freeman, "Bifocal contact lenses having diffractive power." UK Patent application GB 2129157A (10 May 1984).
24. D. A. Atchison and L. N. Thibos, "Diffractive properties of the Diffrax bifocal contact lens," Ophthalm. Physiol. Opt. **13**(2), 186–188 (1993).

Optics EXPRESS

25. M. H. Freeman and J. Stone, "A new diffractive bifocal contact lens," J. Brit. Cont. Lens Ass. **10**(4), 15–22 (1987).
26. V. Moreno, J. F. Román, and J. R. Salgueiro, "High efficiency diffractive lenses: deduction of kinoform profile," Am. J. Phys. **65**(6), 556–562 (1997).
27. L. Clavé, A. Torrents, and M. S. Millan, "Visual acuity at various distances and defocus curve: a good match," Photonics **9**(2), 85 (2022).
28. Y. Le Grand and S. G. El Hage, *Physiological Optics*, (Springer-Verlag Berlin Heidelberg, New York, 1980).
29. L. N. Thibos, M. Ye, X. Zhang, *et al.*, "The chromatic eye: A new reduced-eye model of ocular chromatic aberration in humans," Appl. Opt. **31**(19), 3594–3600 (1992).